Article:
Li, K, Jiang, J, Amann, T et al. (4 more authors) (2020) Evaluation of 1,3-diketone as a novel friction modifier for lubricating oils. Wear, 452-453. 203299. ISSN 0043-1648

https://doi.org/10.1016/j.wear.2020.203299

Evaluation of 1,3-Diketone as a Novel Friction Modifier for Lubricating Oils

Ke Li [a,b,*], *Jinming Jiang* [b,c], *Tobias Amann* [d,**], *Yuyang Yuan* [a,b], *Chun Wang* [e], *Chengqing Yuan* [b,c], *Anne Neville* [e]

a Intelligent Transport Systems Research Center, Wuhan University of Technology, Wuhan, 430063, China.

b Reliability Engineering Institute, National Engineering Research Center for Water Transport Safety, MOST, Wuhan, 430063, China.

c School of Energy and Power Engineering, Wuhan University of Technology, Wuhan 430063, China.

d Fraunhofer Institute for Mechanics of Materials IWM, Freiburg, Germany

e Institute of Functional Surfaces, Department of Mechanical Engineering, University of Leeds, Leeds, United Kingdom

*Corresponding Author: Ke Li. Wuhan University of Technology, Heping Road 1178, Wuhan 430063, China. Email address: li_ke@whut.edu.cn

** Corresponding Author: Tobias Amann. Fraunhofer Institute for Mechanics of Materials IWM, Woehlerstraße 11, Freiburg 79108, Germany. Email address: tobias.amann@iwm.fraunhofer.de

Abstract: With the growing demand in both lubrication performance and environmental protection, it is eager to seek novel lubricant additives of good oil miscibility and high tribological efficiency but without harmful elements such as sulfur and phosphorus. As a recently developed material with superlubricity ($\mu < 0.01$), 1,3-diketone EPND (1-(4-ethyl phenyl) nonane-1,3-dione) could modify the contacts of steel surfaces through the tribochemical reaction with iron and also exploit strong intermolecular forces to control the near surface fluid interactions. Owing to its oil-soluble nature, EPND also shows the potential functioning as an additive in lubricating oils. In this study, EPND was introduced into both pure base oils and fully-formulated oils to evaluate its performance as a novel friction modifier. The results suggest that with small influences on the viscosity and oxidation stability in the blended oil, EPND leads to an effective friction reduction in both boundary and mixed lubrication regimes. Moreover, the addition of EPND enhances the oil extreme pressure capacity as well. This work indicates that 1,3-diketone is a promising friction modifier even in the presence of some other commercial additives.

Keywords: 1,3-diketone; oil-soluble additives; friction reduction; extreme pressure capacity

1 Introduction

Friction is crucial for the energy efficiency and material durability of mechanical systems. The development of complex oil chemistries has been the most effective strategy to reduce friction when metal-metal contact occurs. In recent years, the use of lubricants with lower viscosity has become an important trend to reduce hydrodynamic friction losses[1]. However, in the boundary and mixed lubrication regimes where the lubricating oil cannot form a sufficiently effective film at the interface of friction pairs to prevent direct solid-solid contacts the lubricant chemistry becomes very important. Thus the development of high-performance friction modifiers (i.e. lubricant additives for friction reduction) becomes more and more significant[2].

One class of highly efficient friction modifier is the organomolybdenum compound, such as molybdenum dithiocarbamate (MoDTC)[3] and molybdenum dialkyldithiophosphate (MoDTP)[4]. This class of additive can reduce friction and wear by the formation of a protective film containing MoS_2 and other molybdenum oxides[5]. However, both sulfur and phosphorus are harmful elements for the environmental concern. Ashes formed by molybdenum can also damage the biodegradability of the oil[6]. In the last two decades Ionic liquids (ILs), a novel developed group of lubricant additives such as pyrrolidinium[7], ammonium[8] and imidazolium[9] salts, can effectively form strong adsorption films on the rubbing surfaces due to their high polarity. But their corrosion inhibition and compatibility with other surface-adsorbing additives needs further investigation[10]. In contrast to soluble organic friction modifiers, nanoparticles such as metals[11], metal oxides[12] and carbon materials[13-14] have been developed to manage tribology in mechanical processes such as rolling effect, protective film, mending effect and polishing effect[15]. However, the homogeneity and stability of their dispersion in base oils are still a major challenge for commercial applications[16].

Another novel class of lubricating material is liquid crystals (LCs), which exhibit a mesophase between the liquid and the crystalline phase. Owing to their high polarity and molecular orientation, liquid crystals exhibit attractive tribological properties both as base oil and as lubricant additives[17]. Luo et al.[18-20] found that when a nematic liquid crystal 5CB (4-n-pentyl-4'-cyanobiphenyl) was added to hexadecane, the lubricant film became thicker but the coefficient of friction (COF) was even significantly reduced. This actually contradictory behavior was explained by the thin film lubrication theory where molecules attach themselves to the surface and the shear induces a specific molecular orientation. Gao et al.[21] reported that the adsorption of 5CB on the sliding steel surfaces play an important role in the friction reduction. Itoh et al.[22] also found that the slip of the 5CB layers adjacent to the substrate leads to low friction and high load capacity.

Therefore, the development of effective oil-soluble additives without environmentally harmful elements is of great significance. The additives which have both strong solid-fluid interactions and intermolecular interactions like liquid crystals are especially preferable. In our prior work[23-31] a synthetic 1,3-diketone (1-(4-ethyl phenyl) nonane-1,3-dione) oil (abbreviated as EPND) has been discovered as the first oily material of superlubricity achieved through experimental methods on the macroscopic scale. This molecule exhibits a rod-like structure similar to 5CB and supplies a high intermolecular force like liquid crystals[28]. It can reach an ultralow COF (≈0.005) on steel surfaces after a certain running-in period in both tribological reciprocating[28-31] and rotating[23-27] systems. Its superlubricity is attributed to two effects (Figure 1): (1) Through chelating with iron, the tribochemical reaction between EPND and the steel surface eliminates solid contacts and leads to a full fluid film[30]; (2) The chemisorption of EPND on steel surfaces and its strong intermolecular interactions facilitate the molecular alignment and smaller shear resistance[25, 28].

Although this 1,3-diketone has attracted more and more research interest[32-33] and shows excellent lubricity especially for applications with relatively low contact pressure (e.g. plain bearings[27]), other aspects of a lubricant such as anti-oxidation, oil detergency, low temperature fluidity and extreme pressure capacity must be also taken into account. Moreover, as a synthetic material, its high preparation cost needs to be considered as well for industrial applications. Thus it is meaningful to explore it in the field of lubricant additives. As 1,3-diketone functions mainly via the tribochemical reaction on the steel surface and the control of fluid near the surface, it is reasonable to hypothesize that 1,3-diketone could still work positively at the solid-fluid interface when it is used as additives. It is expected that the addition of a small amount of 1,3-diketone would improve lubrication but not degrade other physical or chemical properties of base oils.

The present work aimed at the performance evaluation of 1,3-diketone functioning as a friction modifier in oils of different viscosities under various operating conditions. Two pure polyalphaolefin (PAO) oils with low (PAO2) and high (PAO8) viscosity were selected as the base oils. To study its performance in the presence of other additives, EPND was also introduced into two commercial fully-formulated oils with the same viscosity as PAO2 and PAO8. The rheological properties, oxidation stability and Stribeck behavior of the prepared hybrid oils were analyzed. Their friction and wear performance in different lubrication regimes and their extreme pressure behavior were assessed.

2 Materials and methods

The studied 1,3-diketone EPND was synthesized via a Claisen condensation reaction, and the detailed synthesis procedure was described in our prior work[30]. Two pure PAO base oils (PAO2 and PAO8 from Exxon Mobil) and two fully-formulated oils (Great Wall 4121, a precision instrument oil from SINOPEC; Summit SH46, an air compressor oil form Kluber) were selected

as the lubricating oils. As the normal content of lubricant additives is less than 5%, the doping concentrations of EPND studied here were 1% and 5% in weight. After the homogenization in an ultrasonic bath for 10 minutes, well-dispersed hybrid oils were prepared, which showed no phase separation for several months.

The dynamic viscosities of studied oils were measured using a rotary rheometer (MCR102, Anton Paar) with a cone-plate geometry. The testing temperatures varied from 20°C to 120°C at a constant shear rate of 1000 s^{-1}. Each sample was tested for five times.

The oxidation stability of studied oils was determined using a differential scanning calorimetry (DSC, Q2000, TA Instruments). The oil samples were heated from ambient temperature (25°C) to 320°C under a flow of oxygen gas (50 mL/min). Due to the exothermic nature of the oxidation reactions, the oxidation of the sample was observed as a sharp increase in the energy flow where the oxidation induction temperature (OIT) was obtained. For each sample the average OIT value of five repeated measurements was recorded.

Friction tests were performed in a rotating ball-on-3-pin geometry (Figure 2a) using the tribological measuring cell of a rotary rheometer (MCR302, Anton Paar) at room temperature (~ 25°C). The contact of the ball (diameter = 12.7 mm, R_a = 0.03 μm, R_z = 0.13 μm) and the pin (diameter × length = 6 × 6 mm, R_a = 0.2 μm, R_z = 1.43 μm), both made of bearing steel (GB GCr15, i.e. DIN 100Cr6), was always immersed by the tested oil. The oil behavior was analyzed by plotting a Stribeck diagram from the speed of 1 mm/s to 1400 mm/s at a constant load of 0.5 N (i.e. the maximum contact pressure of 317 MPa). The 1-hour duration friction tests were performed under 0.5 N load at 100 mm/s and 1000 mm/s respectively. All friction tests were repeated five times.

The worn morphology of all tested ball and pin specimens were analyzed using a laser microscope (VK-X1000, Keyence). The worn volume of pin specimens was calculated by the equipment software itself.

The oil extreme pressure (EP) behavior was examined by a 4-ball tribometer (Figure2b, MFT-4BM, Rtec-Instruments) according to the GB12583 standard (similar to ASTM D-2783). At room temperature (~25°C), a series of tests were made at 1760 rpm for 10 seconds under certain increasing specified loads (e.g. 431 N, 461 N, 490 N, 510 N and so on). Once the generated wear scar diameter under which load (e.g 490 N) exceeded 5% of the specified value under this load, it indicated the occurrence of the seizure and the former load (e.g. 461 N in this case) was considered as the maximum non-seizure load (P_B). Each oil sample was tested five times, in which the measured wear scar diameters showed a little bit different but it was found that they all referred to the same specified P_B level according to the GB12583 standard.

3 Results and Discussion

3.1 Rheological Properties and Oxidation Stability

The viscosity-temperature curves of studied oils measured using the rheometer are illustrated in Figure 3. Since the doping contents were only 1% and 5%, the addition of EPND did not obviously affect the viscosity of the original oils in the entire testing temperature range from 20°C to 120°C. Since all subsequent tribological tests were carried out at room temperature, a comparison of viscosity values at 25°C is also shown in Figure 4. EPND has a very similar viscosity (7 mPa·s) to PAO2 and 4121, so its incorporation has no influence on the viscosity of this low viscous (LV) group. As for the high viscous (HV) group (i.e. PAO8 and SH46), owing to the much bigger viscosity difference the viscosity reduction of hybrid oils was measurable. For instance, compared

to SH46, the viscosity of SH46+5%EPND was decreased by 6% from 78 mPa·s to 73 mPa·s, which might consequently influence their tribological performance.

The oxidation stability of lubricating oils was measured using DSC. Figure 5 describes the DSC curves of PAO2, 4121 and EPND as the example. As a fully-formulated oil, 4121 probably contains anti-oxidation additives and shows the best oxidation stability with an OIT of 228.8°C. EPND has a lower OIT (179.6°C) than that of PAO2 (202.7°C) may be due to the unsaturation of its carbonyl groups. The second exothermal peak of EPND might be attributed to the enol form tautomer of 1,3-diketone, which has an intramolecular hydrogen bond with better stability than the keto form tautomer[29]. Figure 6 summarizes the OITs of all studied lubricating oils. It suggests that the degradation of oxidation stability induced by the incorporation of EPND was small. The biggest difference in OIT was between sample SH46 and SH46+5% EPND, which was still less than 10°C.

3.2 Tribological Performance

Figure 7 depicts the Stribeck curves of studied oils measured by the ball-on-3-pin tribological cell. To make the curve cover more regions of different lubrication regimes, a very small load (0.5 N) and a very wide velocity range (1 ~ 1400 mm/s) were applied. Since the tribochemical reaction between EPND and steel could change the contact morphology and contact pressure of two sliding surfaces[30], a very short testing time (40 s) was used in each Stribeck measurement. In this way the influence of the change in friction pairs was eliminated and it was assumed that all the obtained curves were just due to the properties of the oil itself.

Figure 7a shows that although EPND has a similar viscosity to PAO2, it behaved a much lower COF value than PAO2 over the entire speed range. This result shows a good agreement with the previous study using a ball-on-disc rotating measurement[25], which is attributed to the surface-

adsorption (proved by both X-ray photoelectron spectrometry and time-of-flight secondary ion mass spectrometry[23]) and molecular alignment (revealed by both molecular dynamic simulations[28] and shear-thinning behavior[25]) of EPND like the "smart lubrication" of 5CB proposed by Nakano et al.[34-36]. When EPND was introduced into the LV group (Figure 7a and 7b), in PAO2 1% EPND made a change at lower velocity of < 600 mm/s but for 5% there was a change across almost all velocities. For 4121 there was no change at 1% at all and at 5% a small change at < 500 mm/s, indicating that other additives in 4121 may have an effect. In general, the introduction of EPND led to the friction reduction, especially at low velocities. The reason is when the hydrodynamic effect is weak, EPND has better ability to form the oil film. This point has been witnessed by the thicker film thickness of 1,3-diketone than PAO2 at low velocities measured using a relative optical interference intensity method[23].

However, the situation for the HV group (Figure 7c and 7d) was quite different. The incorporation of EPND increased the friction in the boundary lubrication regime (e.g. 100 mm/s) and decreased the friction in the hydrodynamic lubrication regime (e.g. 1000 mm/s). Compared to the LV group, the viscosity change caused by EPND played a more important role. The performance of the HV group followed the regular correlation of viscosity, velocity and COF, i.e. the oil with lower viscosity behaves higher COF at low velocities and lower COF at high velocities.

To investigate the long-term performance of studied oils, 1-hour duration friction tests were operated under the load of 0.5 N at constant speeds (Figure 8). Based on the results in the Stribeck test, hybrid oils with 5% EPND were selected and measured to show a more obvious influence of the 1,3-diketone additive on the COF. In order to analyze its performance in different lubrication regimes, the friction tests were operated at both velocities of 100 mm/s and 1000 mm/s. The wear scars of all pin specimens after the friction tests were observed using a laser microscope and the

wear volume of each pin was calculated by the software (Figure 9a). The total wear volume of the three pins from each test is summarized in Figure 10.

For the LV group, the COF of PAO2 and 4121 kept nearly constant during the test at both 100 mm/s and 1000 mm/s (Figure 8a and 8b). When 5% EPND was applied, a running-in process could be found accompanied with the reduction of friction and the increase of wear. This phenomenon was more obvious at 100 mm/s (e.g. the maximum COF reduction was more than 50% in the case of 4121 at 100 mm/s), presumably because the solid-solid contact was more severe and the induced asperity flash temperature supplied more energy for the tribochemical reaction between 1,3-diketone and steel surfaces, which has been proved to be thermally activated in our prior work[30]. Here it should be also noted that although the introduction of EPND generated more wear, this tribochemical process could be stopped automatically as soon as the contact pressure was lowered enough to allow the separation of sliding surfaces by a lubricant film. Prior work has proved that the ultralow friction (COF = 0.005) of pure EPND can be maintained for more than 100 hours and the wear is self-limited after the running-in period[30]. In practical applications, low viscous oils such as 4121 are mainly used for the lubrication of precision instruments, which normally work at low loads/high speeds and place very high demands on the minimization of friction. Hence in view of long-term operation or even lifetime lubrication the friction reduction induced by EPND will be extremely beneficial and the "sacrificial" wear during the running-in will be self-limited.

For the HV group, when the sliding velocity of 100 mm/s was applied (Figure 8c), although PAO8+5%EPND and SH46+5%EPND have lower viscosity than their original oils, the tribochemical reaction of EPND still resulted in a lower COF. As this running-in process was very short (~20 minutes), the generated wear scars were too shallow to calculate their wear volume (Figure 9b). In the case of 1000 mm/s (Figure 8d), all tested oils show constant COF values. The

slightly lower friction of PAO8+5%EPND and SH46+5%EPND might be mainly due to their lower viscosity (i.e. smaller shear resistance). Similarly, the wear volume of their scars were also very small and undetectable.

Unlike the LV group, the HV group is usually applied in the operating conditions with relatively high load and low speed. For instance, SH46 is a typical lubricating oil for the screws of air compressors, in which the extreme pressure capacity is an important property. Therefore, the maximum non-seizure load (P_B) values of the HV group were measured according to the referred standard using a 4-ball tribometer. After tested under a certain load for 10 s, the balls were analyzed by the laser microscope (Figure 11). Once seizure occurred, a dramatical increase of the wear scar diameter cloud be observed. The P_B values of tested oils are summarized in Figure 12. Owing to its EP additives, SH46 showed much higher P_B (618 N) than the one of PAO8 (431 N). When 5% EPND was added, the P_B values were enhanced to 696 N in SH46 and to 530 N in PAO8 respectively. This improvement should be due to the strong surface adsorption of EPND, which effectively enhances the resilience of the base oil.

4 Conclusions

The present work investigated the lubrication improvement of 1,3-diketone EPND as a novel friction modifier for lubricating oils. Its influences on oil viscosity, oxidation stability, Stribeck behavior, friction/wear and extreme pressure capacity were evaluated. The main conclusions drawn from the results are as follows:

- EPND is preferable to be blended into oils with similar low viscosity such as PAO2, because the range of incorporation ratio could be wide without the concern of viscosity

change. However, when EPND is introduced into high viscous oil the viscosity change needs to be considered.

- Although EPND itself shows a little worse oxidation stability than PAO base oil, it has a very small influence in the blended oil when applied as a lubricant additive.
- In the boundary lubrication regime EPND functions mainly through the tribochemical reaction, in which the friction reduction and the acceptable "sacrificial" wear needs to be carefully balanced; in the mixed lubrication regime EPND functions mainly via its surface-adsorption and molecular alignment; in the hydrodynamic lubrication regime the effect of EPND is small.
- Owing to its strong adherence on steel surfaces, EPND could also greatly enhance the oil extreme pressure capacity.
- Although the composition of existing additives in 4121 and SH46 are unknown, no obvious antagonism for EPND have been found. In the future work other aspects such as oil detergency, anti-corrosion and low temperature fluidity should be further studied to explore optimal formulated oils.

Acknowledgments: This work was supported by the National Natural Science Foundation of China (No. 51975437 and No. 51605351).

References

[1]. Guegan, J.; Southby, M.; Spikes, H., Friction Modifier Additives, Synergies and Antagonisms. *Tribol. Lett.* **2019,** *67* (3), 12.

[2]. He, X. L.; Lu, J.; Desanker, M.; Invergo, A. M.; Lohr, T. L.; Ren, N.; Lockwood, F. E.; Marks, T. J.; Chung, Y. W.; Wang, Q. J., Boundary Lubrication Mechanisms for High-Performance Friction Modifiers. *Acs Applied Materials & Interfaces* **2018,** *10* (46), 40203-40211.
[3]. De Feo, M.; Bouchet, M. I. D. B.; Minfray, C.; Esnouf, C.; Le Mogne, T.; Meunier, F.; Yang, L.; Thiebaut, B.; Pavan, S.; Martin, J. M., Formation of interfacial molybdenum carbide for DLC lubricated by MoDTC: Origin of wear mechanism. *Wear* **2017,** *370*, 17-28.
[4]. Wang, W.; Li, C.; Yang, J.; Shen, Y.; Xu, J., Friction performance of MoDTP and ester-containing lubricants between CKS piston ring and cast iron cylinder liner. *Lubrication Science* **2018,** *30* (1), 33-43.
[5]. Tang, Z.; Li, S., A review of recent developments of friction modifiers for liquid lubricants (2007-present). *Current Opinion in Solid State & Materials Science* **2014,** *18* (3), 119-139.
[6]. Xu, X.; Li, J.; Sun, L.; Xue, Q., Tribological study of borated hydroxyalkyldithiocarbamate as additive for environmentally adapted lubricants. *Industrial Lubrication and Tribology* **2013,** *65* (1), 19-26.
[7]. Monge, R.; Gonzalez, R.; Hernandez Battez, A.; Fernandez-Gonzalez, A.; Viesca, J. L.; Garcia, A.; Hadfield, M., Ionic liquids as an additive in fully formulated wind turbine gearbox oils. *Wear* **2015,** *328*, 50-63.
[8]. Oulego, P.; Blanco, D.; Ramos, D.; Viesca, J. L.; Diaz, M.; Hernandez Battez, A., Environmental properties of phosphonium, imidazolium and ammonium cation-based ionic liquids as potential lubricant additives. *Journal of Molecular Liquids* **2018,** *272*, 937-947.
[9]. Yang, X.; Meng, Y.; Tian, Y., Effect of Imidazolium Ionic Liquid Additives on Lubrication Performance of Propylene Carbonate under Different Electrical Potentials. *Tribol. Lett.* **2014,** *56* (1), 161-169.
[10]. Zhou, Y.; Qu, J., Ionic Liquids as Lubricant Additives: A Review. *Acs Applied Materials & Interfaces* **2017,** *9* (4), 3209-3222.
[11]. Zhang, C.; Zhang, S.; Song, S.; Yang, G.; Yu, L.; Wu, Z.; Li, X.; Zhang, P., Preparation and Tribological Properties of Surface-Capped Copper Nanoparticle as a Water-Based Lubricant Additive. *Tribol. Lett.* **2014,** *54* (1), 25-33.
[12]. Xu, Y.; Zheng, Q.; Geng, J.; Dong, Y.; Tian, M.; Yao, L.; Dearn, K. D., Synergistic effects of electroless piston ring coatings and nano-additives in oil on the friction and wear of a piston ring/cylinder liner pair. *Wear* **2019,** *422*, 201-211.
[13]. Saurin, N.; Aviles, M. D.; Espinosa, T.; Sanes, J.; Carrion, F. J.; Bermudez, M. D.; Iglesias, P., Carbon nanophases in ordered nanofluid lubricants. *Wear* **2017,** *376*, 747-755.
[14]. Xu, Y.; Peng, Y.; Dearn, K. D.; Zheng, X.; Yao, L.; Hu, X., Synergistic lubricating behaviors of graphene and MoS2 dispersed in esterified bio-oil for steel/steel contact. *Wear* **2015,** *342*, 297-309.
[15]. Lee, K.; Hwang, Y.; Cheong, S.; Choi, Y.; Kwon, L.; Lee, J.; Kim, S. H., Understanding the Role of Nanoparticles in Nano-oil Lubrication. *Tribol. Lett.* **2009,** *35* (2), 127-131.
[16]. Shahnazar, S.; Bagheri, S.; Abd Hamid, S. B., Enhancing lubricant properties by nanoparticle additives. *International Journal of Hydrogen Energy* **2016,** *41* (4), 3153-3170.
[17]. Carrion, F.-J.; Martinez-Nicolas, G.; Iglesias, P.; Sanes, J.; Bermudez, M.-D., Liquid Crystals in Tribology. *International Journal of Molecular Sciences* **2009,** *10* (9), 4102-4115.
[18]. Zhang, S.; Qiao, Y.; Liu, Y.; Ma, L.; Luo, J., Molecular behaviors in thin film lubrication-Part one: Film formation for different polarities of molecules. *Friction* **2019,** *7* (4), 372-387.

[19]. Gao, M.; Li, H. Y.; Ma, L. R.; Gao, Y.; Ma, L. W.; Luo, J. B., Molecular behaviors in thin film lubrication-Part two: Direct observation of the molecular orientation near the solid surface. *Friction* **2019,** *7* (5), 479-488.
[20]. Shen, M. W.; Luo, J. B.; Wen, S. Z.; Yao, J. B., Nano-tribological properties and mechanisms of the liquid crystal as an additive. *Chin. Sci. Bull.* **2001,** *46* (14), 1227-1232.
[21]. Gao, Y.; Xue, B.; Ma, L.; Luo, J., Effect of liquid crystal molecular orientation controlled by an electric field on friction. *Tribology International* **2017,** *115*, 477-482.
[22]. Itoh, S.; Imura, Y.; Fukuzawa, K.; Zhang, H. D., Anisotropic Shear Viscosity of Photoaligned Liquid Crystal Confined in Submicrometer-to-Nanometer-Scale Gap Widths Revealed with Simultaneously Measured Molecular Orientation. *Langmuir* **2015,** *31* (41), 11360-11369.
[23]. Zhang, S.; Zhang, C.; Chen, X.; Li, K.; Jiang, J.; Yuan, C.; Luo, J., XPS and ToF-SIMS analysis of the tribochemical absorbed films on steel surfaces lubricated with diketone. *Tribology International* **2019,** *130*, 184-190.
[24]. Liu, D.; Li, K.; Zhang, S.; Amann, T.; Zhang, C.; Yan, X., Anti-spreading behavior of 1,3-diketone lubricating oil on steel surfaces. *Tribology International* **2018,** *121*, 108-113.
[25]. Li, K.; Zhang, S.; Liu, D.; Amann, T.; Zhang, C.; Yuan, C.; Luo, J., Superlubricity of 1,3-diketone based on autonomous viscosity control at various velocities. *Tribology International* **2018,** *126*, 127-132.
[26]. Amann, T.; Kailer, A.; Oberle, N.; Li, K.; Walter, M.; List, M.; Rühe, J., Macroscopic Superlow Friction of Steel and Diamond-Like Carbon Lubricated with a Formanisotropic 1,3-Diketone. *ACS Omega* **2017,** *2* (11), 8330-8342.
[27]. Amann, T.; Kailer, A.; Beyer-Faiss, S.; Stehr, W.; Metzger, B., Development of sintered bearings with minimal friction losses and maximum life time using infiltrated liquid crystalline lubricants. *Tribology International* **2016,** *98*, 282-291.
[28]. Li, K.; Amann, T.; List, M.; Walter, M.; Moseler, M.; Kailer, A.; Rühe, J., Ultralow friction of steel surfaces using a 1,3-diketone lubricant in the thin film lubrication regime. *Langmuir* **2015,** *31* (40), 11033-11039.
[29]. Walter, M.; Amann, T.; Li, K.; Kailer, A.; Ruehe, J.; Moseler, M., 1,3-Diketone Fluids and Their Complexes with Iron. *Journal of Physical Chemistry A* **2013,** *117* (16), 3369-3376.
[30]. Li, K.; Amann, T.; Walter, M.; Moseler, M.; Kailer, A.; Rühe, J., Ultralow Friction Induced by Tribochemical Reactions: A Novel Mechanism of Lubrication on Steel Surfaces. *Langmuir* **2013,** *29* (17), 5207-5213.
[31]. Amann, T.; Kailer, A., Ultralow Friction of Mesogenic Fluid Mixtures in Tribological Reciprocating Systems. *Tribol. Lett.* **2010,** *37* (2), 343-352.
[32]. Chen, H.; Xu, C.; Xiao, G.; Chen, Z.; Yi, M., Ultralow Friction Between Steel Surfaces Achieved by Lubricating with Liquid Crystal After a Running-in Process with Acetylacetone. *Tribol. Lett.* **2018,** *66* (2), 68.
[33]. Chen, H.; Xu, C.; Xiao, G.; Chen, Z.; Yi, M.; Zhang, J., Effect of Running-In Induced Groove-Structured Wear and Fe(acac)(3) on Ultralow Friction When Lubricating with 5CB Liquid Crystal. *Tribol. Lett.* **2019,** *67* (2).
[34]. Tadokoro, C.; Nihira, T.; Nakano, K., Minimization of Friction at Various Speeds Using Autonomous Viscosity Control of Nematic Liquid Crystal. *Tribol. Lett.* **2014,** *56* (2), 239-247.
[35]. Nakano, K., Scaling law on molecular orientation and effective viscosity of liquid-crystalline boundary films. *Tribol. Lett.* **2003,** *14* (1), 17-24.

[36]. Nakano, K., An investigation into the molecular orientation of sheared liquid crystalline boundary films. *Lubrication Science* **2003,** *15* (3), 233-252.

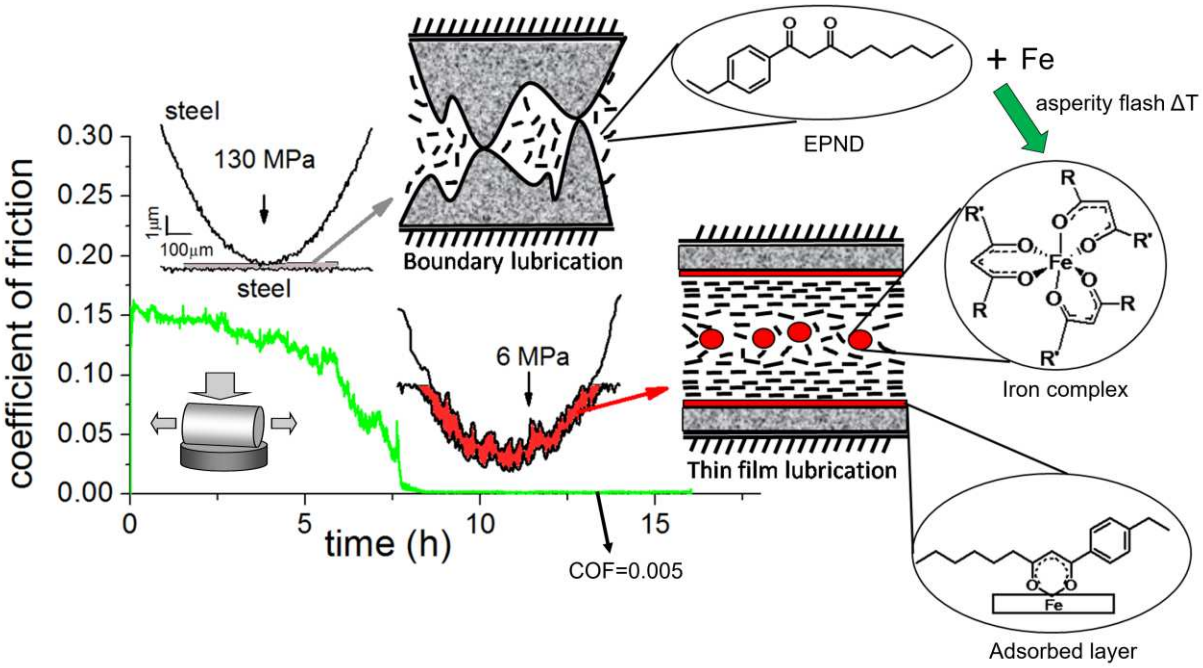

Figure 1. Superlubricity of 1,3-diketone EPND on steel surfaces in a tribological reciprocating system (50 N, 50 Hz, 1 mm, 90°C), adapted from Ref. [28] and [30].

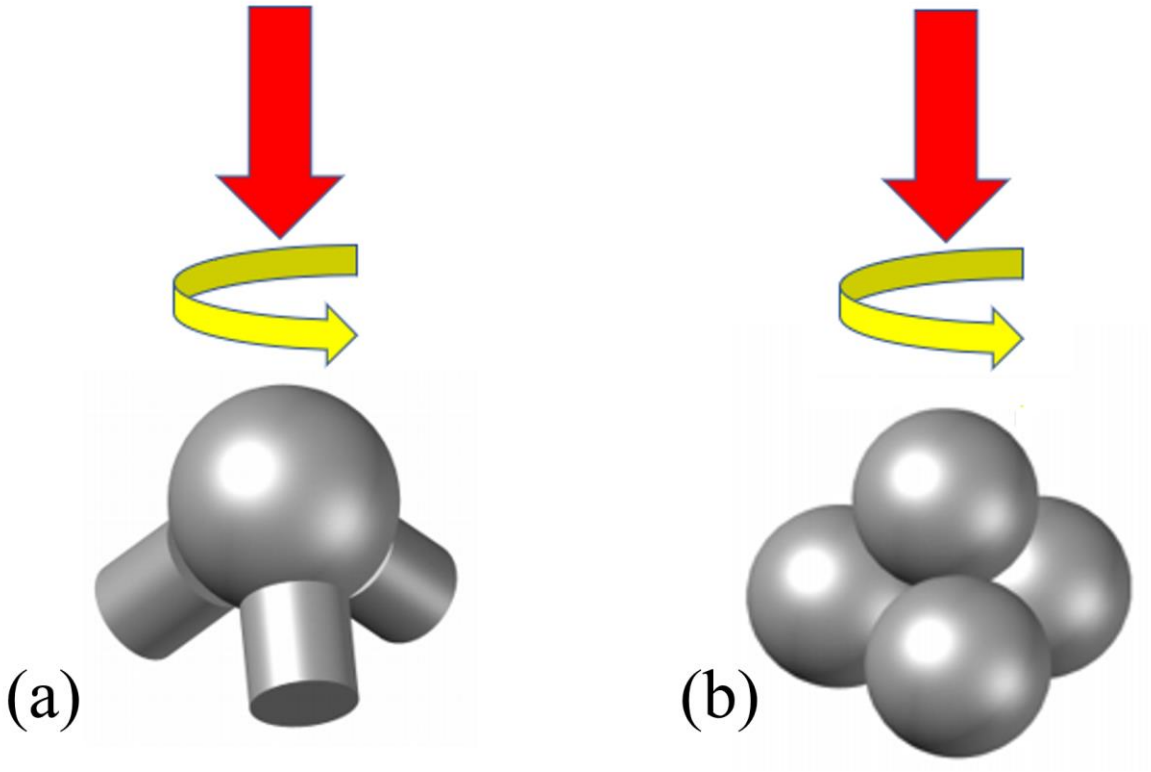

Figure 2. (a) A ball-on-3-pin tribological cell for Stribeck curves measurements and 1-hour duration friction tests. (b) A 4-ball tribometer for extreme pressure capacity measurements.

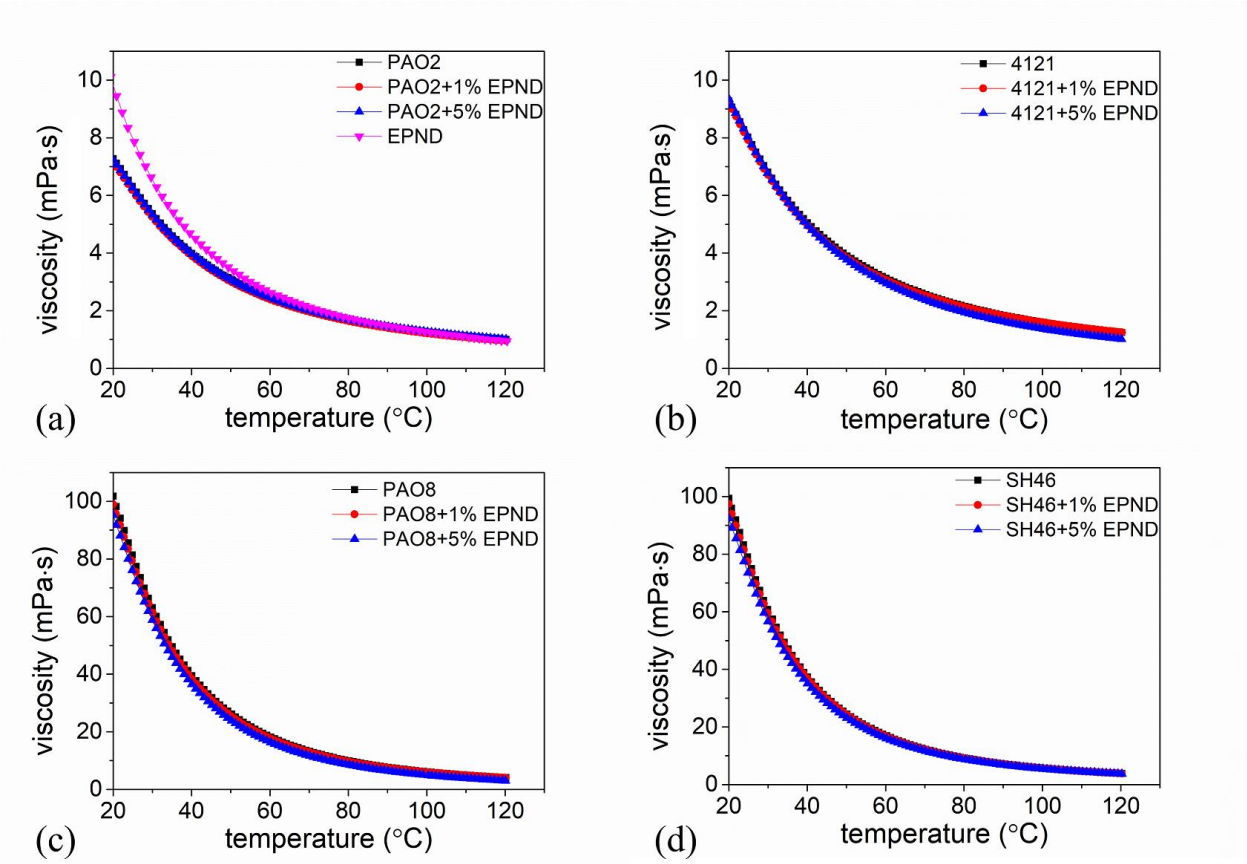

Figure 3. Viscosity-temperature curves of studied oils.

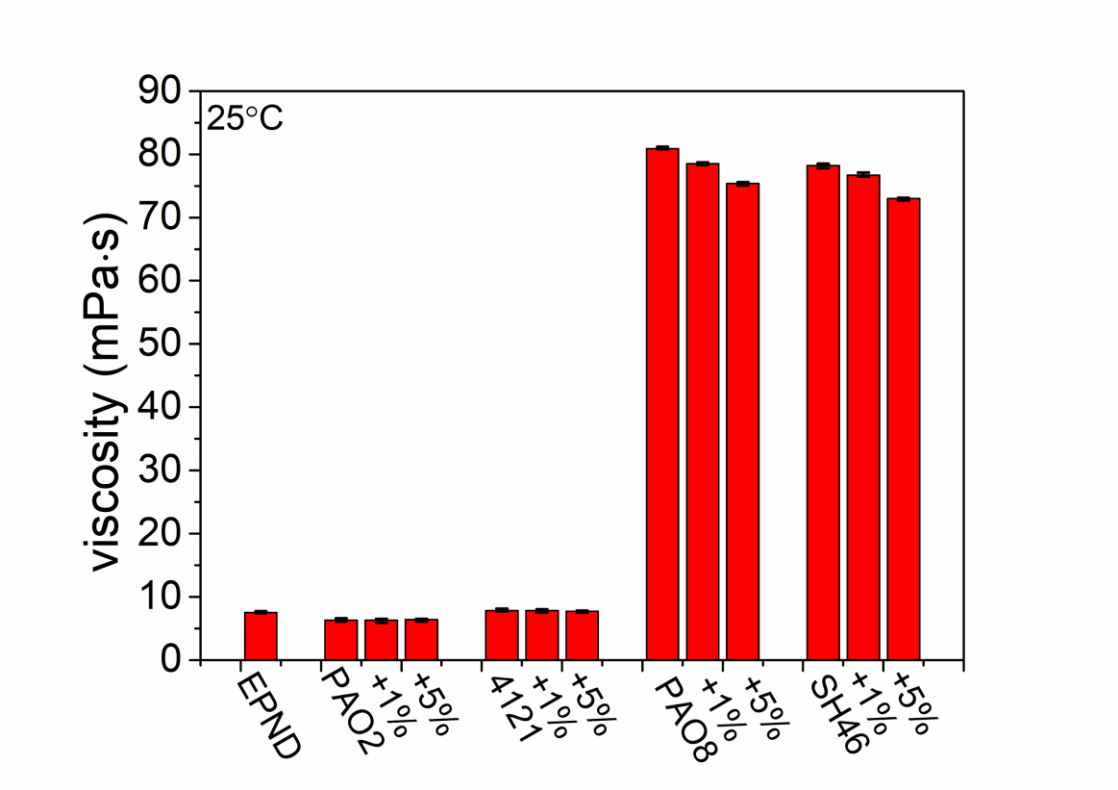

Figure 4. Viscosities of studied oils at 25°C.

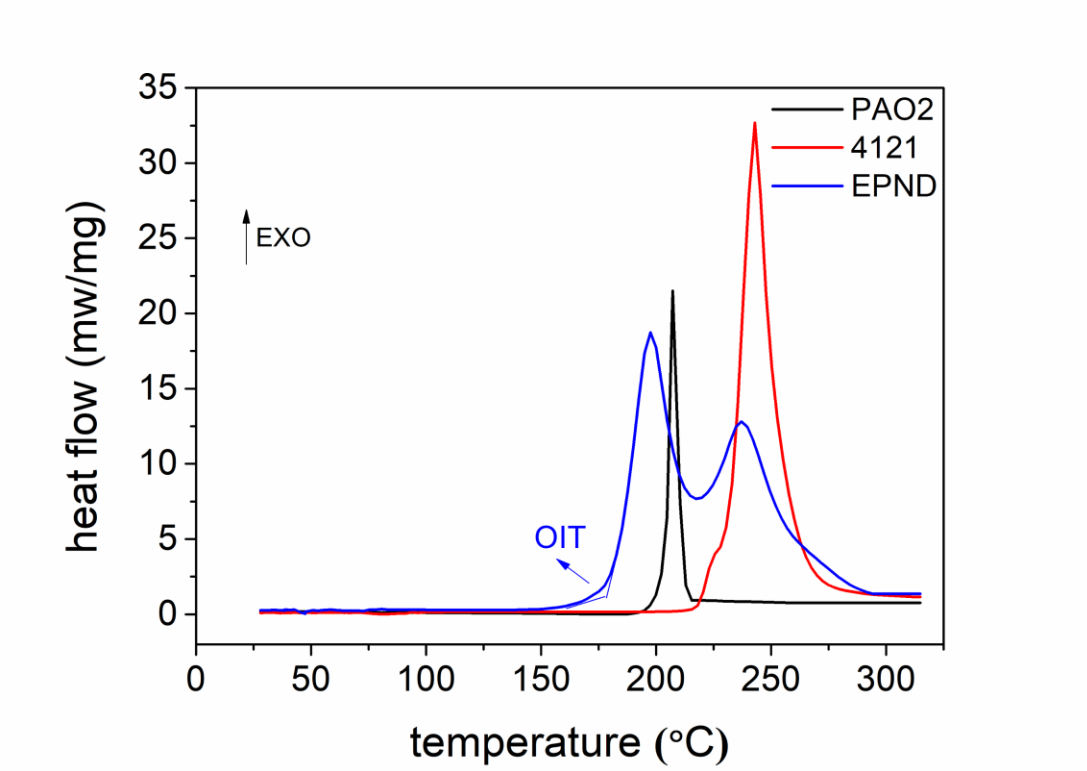

Figure 5. DSC curves of PAO2, 4121 and EPND for measuring their oxidation induced temperatures (OITs).

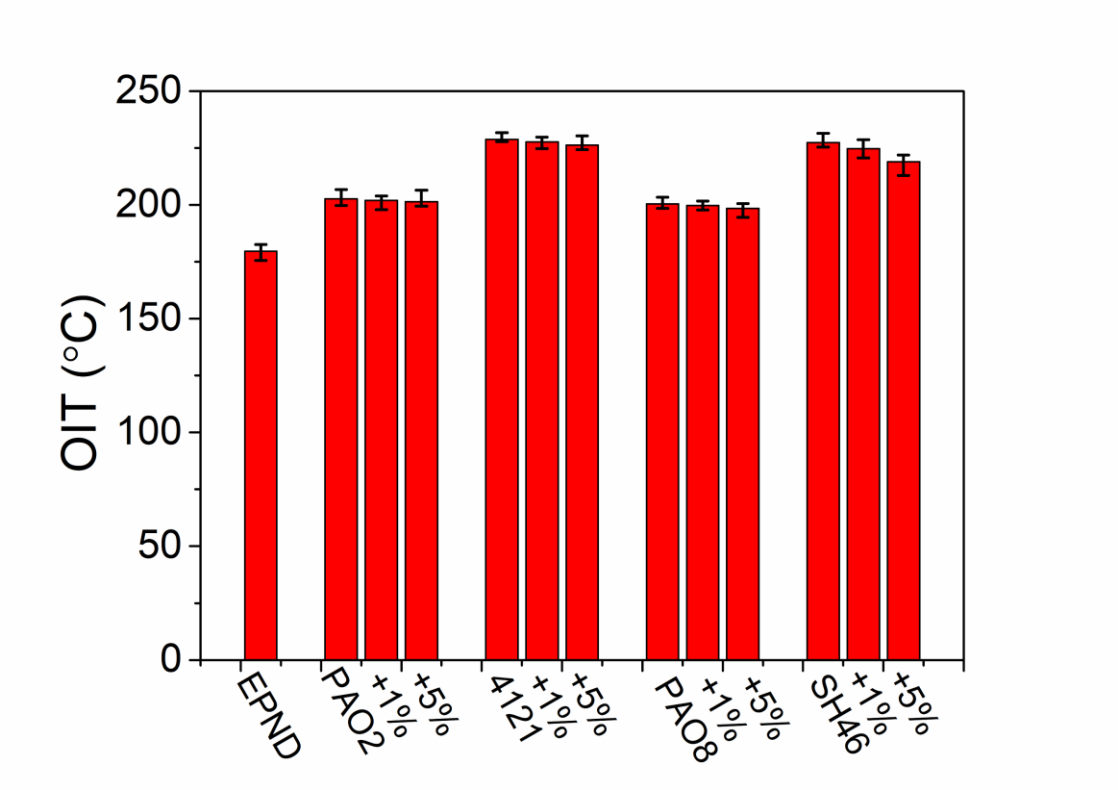

Figure 6. Oxidation induced temperatures of studied oils.

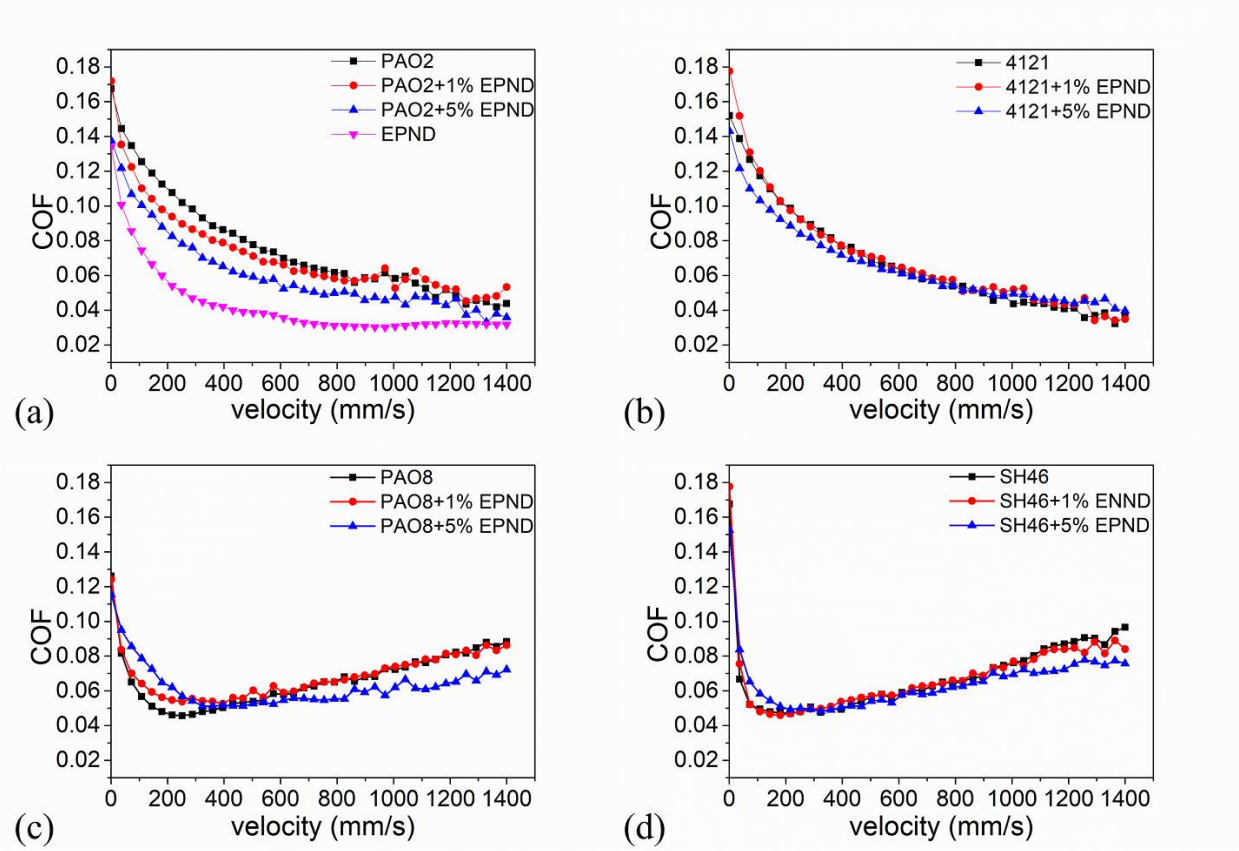

Figure 7. Stribeck curves of studied oils from 1 mm/s to 1400 mm/s (0.5N and 25°C).

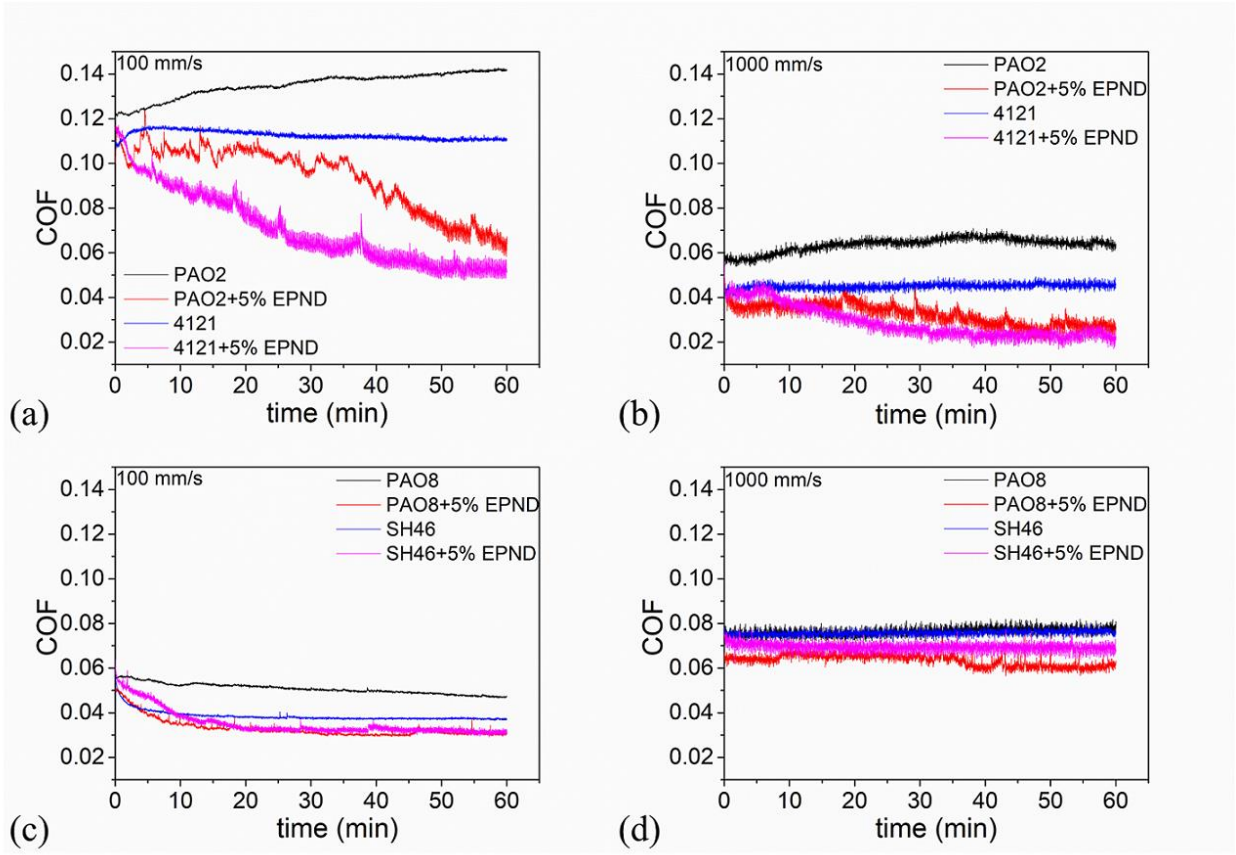

Figure 8. 1-hour duration friction tests of studied oils at 100 mm/s (a and c) and at 1000 mm/s (b and d).

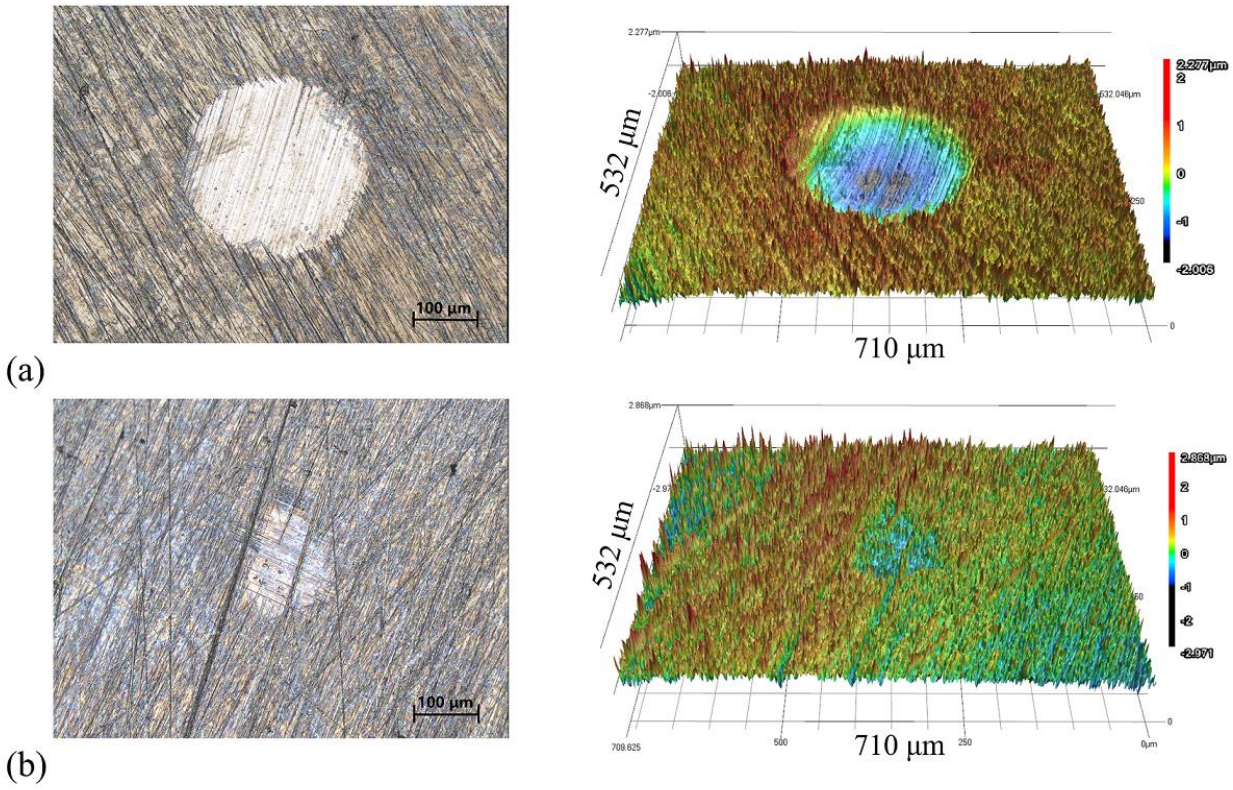

Figure 9. Illustration of pins after 1-hour duration friction tests with detectable wear volume (a) and undetectable wear volume (b).

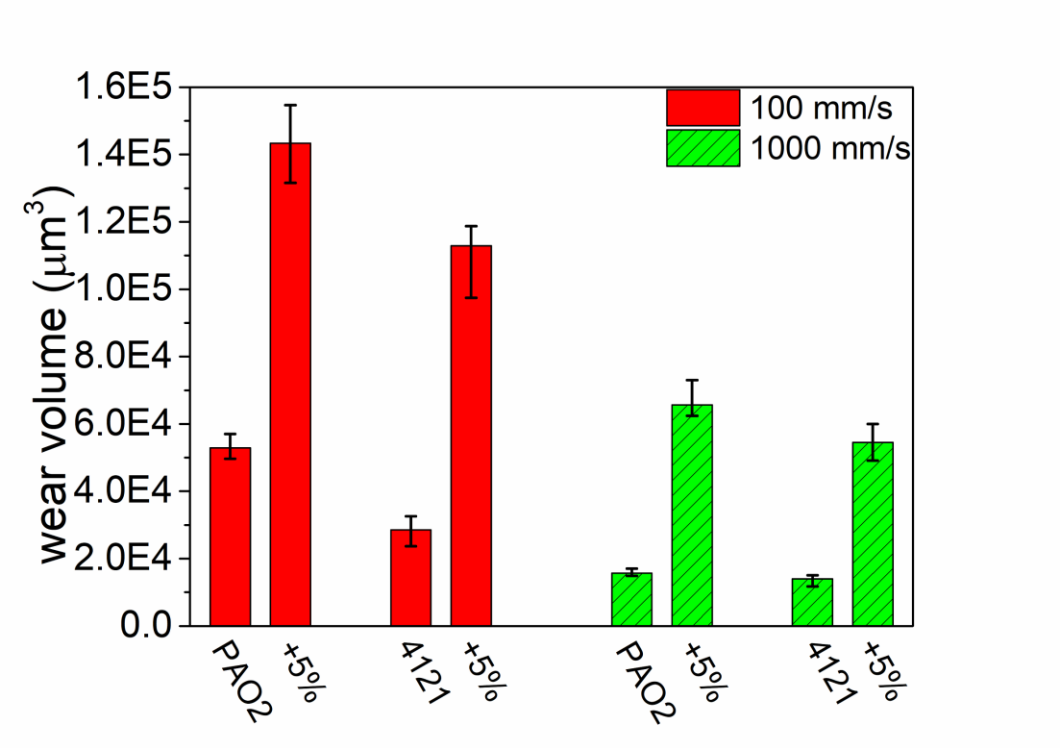

Figure 10. Total wear volume of three pins after 1-hour friction test (the wear volume value of all samples in the HV group were undetectable).

(a) 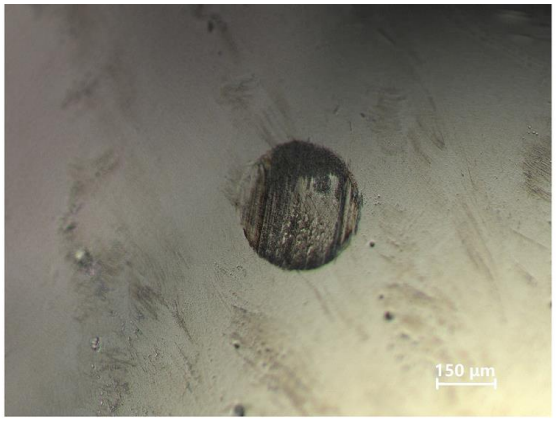

(b) 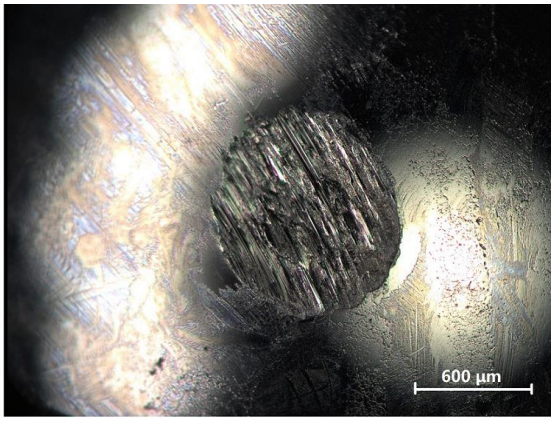

Figure 11. Illustration of balls after 4-ball tests without seizure (a) and when seizure occurred (b).

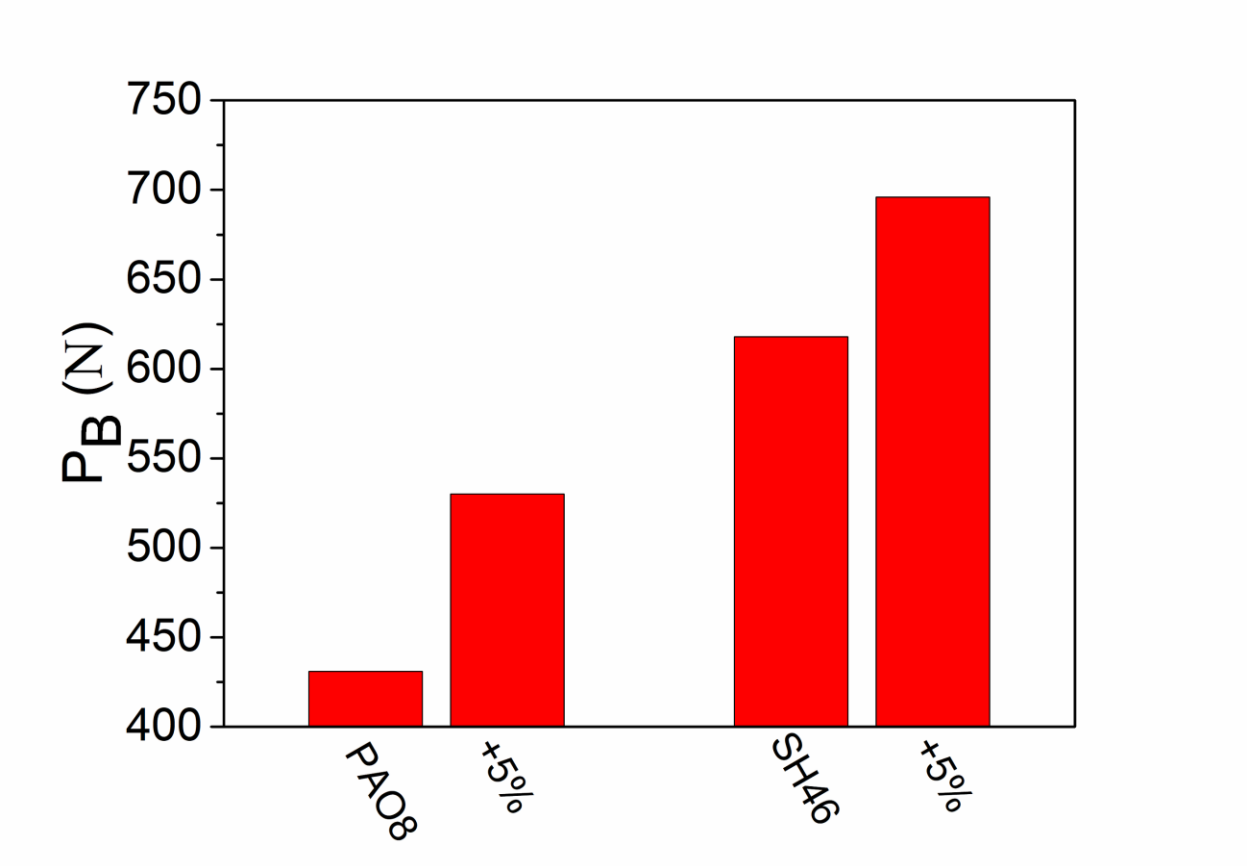

Figure 12. Maximum non-seizure load (P_B) values of the HV group.